Universiteit
Leiden
The Netherlands

Diseases of the nervous system associated with calcium channelopathies

Todorov, B.B.

Citation
Todorov, B. B. (2010, June 2). *Diseases of the nervous system associated with calcium channelopathies*. Retrieved from https://hdl.handle.net/1887/15580

Version:	Corrected Publisher's Version
License:	Licence agreement concerning inclusion of doctoral thesis in the Institutional Repository of the University of Leiden
Downloaded from:	https://hdl.handle.net/1887/15580

Note: To cite this publication please use the final published version (if applicable).

ABLATION OF $CA_V2.1$ CHANNELS IN CEREBELLAR GRANULE CELLS AFFECTS PURKINJE CELL FIRING REGULARITY WITHOUT CAUSING MOTOR DISCOORDINATION

Freek E. Hoebeek [1], Boyan Todorov[2], Elisa Galliano[1,4], A. Pop[1], Zhenyu Gao[1], Martijn Schonewille[1], Egidio D'Angelo[4], Arn M.J.M. van den Maagdenberg [2,3], and Chris I. De Zeeuw [1,5]

[1]Departments of Neuroscience, Erasmus MC Rotterdam, Rotterdam, The Netherlands; Departments of [2]Human Genetics and [3]Neurology, Leiden University Medical Center, Leiden, The Netherlands; [4]Department of Cellular-Molecular Physiological and Pharmacological Sciences, University of Pavia, Italy; [5]Netherlands Institute for Neuroscience, Royal Dutch Academy for Sciences, Amsterdam, The Netherlands

Manuscript in preparation

ABSTRACT

Although cerebellar granule cells account for nearly half the number of neurons in the central nervous system, their role in motor coordination remains elusive. Their projections - either directly via parallel fibers or indirectly via interneurons of the molecular layer - reach Purkinje cells and influence their activity. Neurotransmission from the granule cells depends on the action of $Ca_V2.1$ channels. Reduced $Ca_V2.1$ channel activity is known to affect the firing behavior of cerebellar Purkinje cells, which compromises their modulatory role in motor control. However, since $Ca_V2.1$ channels are heavily expressed in all layers of the cerebellar cortex, it is difficult to assess the exact contribution of granule cells. Here, we used a genetic approach to investigate the role of these cells in regulating Purkinje cell firing patterns in relation to motor behavior. To this end, we generated *Cacna1a* knockout (KO) mice that do not have functional $Ca_V2.1$ channels in cerebellar granule cell neurons. This was achieved by crossing *Cacna1a* conditional mice with mice expressing Cre-recombinase under the control of the granule cell-specific $GABA_A$ receptor α6-promoter. The $\alpha6^{Cre}$-*Cacna1a* KO mice show no overt structural abnormalities in the cerebellum nor signs of motor coordination problems, despite strongly reduced neurotransmission at parallel fiber–Purkinje cell synapses. Purkinje cells of KO mice have a normal overall simple spiking frequency, but a decreased irregularity in their firing pattern. To study the consequence of this change on motor behavior, mice were subjected to various motor tasks, all of which showed no difference between KO and wild-type mice, except for vestibulo-ocular reflex (VOR) learning paradigms, which test for compensatory eye movements. While KO mice are perfectly able to decrease their VOR gain, they forget the newly learned compensatory eye movements overnight, indicating that the consolidation of motor learning is affected. These results indicate that the presence of $Ca_V2.1$ channels in granule neurons is important for ensuring the irregularity of Purkinje cell firing pattern and for the consolidation of motor learning in KO mice.

INTRODUCTION

The cerebellum is known to play an important role in fine-tuning motor coordination. To perform its role, the cerebellum receives sensory and cortical input through mossy fibers. Mossy fibers originate from various precerebellar nuclei and their projections reach the granule cell neurons in the cerebellar cortex (*Glickstein, 1997*). Granule cells transmit this information further to Purkinje cells via their ascending axons and the parallel fiber pathway, providing excitatory input either directly or indirectly via inhibitory interneurons (i.e., stellate and basket cells) of the molecular layer (for review, see *Voogd & Glickstein, 1998*). Purkinje cells are also innervated by climbing fiber originating from neurons in the inferior olive. In response to synaptic input, Purkinje cells generate action potentials. Action potentials are called complex spikes when fired following the activation of a climbing fiber, or simple spikes after parallel fiber activation. Simple spikes are fired constantly at relatively high frequencies (~50 Hz) in awake animals (*Goossens et al., 2004*; *Hoebeek et al., 2005*; *Schonewille et al., 2006*). Simple spiking activity is modulated by the inhibitory interneuron input and the intrinsic excitability of the Purkinje cells themselves (*Llinas & Sugimori, 1980*). When only the parallel fiber-to-Purkinje cell synaptic transmission is blocked Purkinje cells cease to fire simple spikes (*Wada et al., 2007*). This is presumably due to the tonic inhibitory activity of the molecular layer interneurons (*Midtgaard et al., 1992*) that silences the intrinsic activity of the Purkinje cell. This inhibitory input has important physiological role as it is thought to mediate the pauses in Purkinje cells firing (*Hausser & Clark, 1997; Wulff et al., 2009*).

Simple spike firing of Purkinje cells is irregular (i.e., *noise level*), with bursts of spiking and pauses in activity, that are thought to contain essential information for controlling motor behavior (*Steuber et al., 2007; Hoebeek et al., 2008*). In various studies of mouse mutants with motor coordination dysfunction an increased noise level of simple spiking activity was observed that seemed to be determined by: (1) alterations in the intrinsic firing of Purkinje cells themselves (*Hoebeek et al., 2005; Walter et al., 2006*); (2) alterations in the strength of inhibitory input from interneurons of the molecular layer (*Mittmann et al., 2005; Wulff et al., 2009*); and (3) alterations in the strength of excitatory synaptic input from the parallel fibers (*Matsushita et al., 2002; Liu & Friel, 2008*). As most of the mice in these studies had a mutation in $Ca_V2.1$ channel subunits, it appears that these channels are involved in regulating the noise level in Purkinje cell firing.

Voltage-gated $Ca_V2.1$ channels, which play a crucial role in neurotransmission, are highly expressed in cerebellar Purkinje (*Llinas et al., 1989*) and granule (*Zhang et al., 1993*) cells and are important for cerebellar functioning. Several mouse mutants with $Ca_V2.1$ channel gene mutations, such as the $Ca_V2.1$-α_1 subunit-encoding *Cacna1a* mutants *tottering, rolling Nagoya* and *leaner* (*Fletcher et al., 1996; Wakamori et al.,* 1998; *Mori et al., 2000;*) and the $\alpha_2\delta$–2 auxiliary subunit-encoding *Cacd2d2* mutant

ducky (Barclay et al., 2001), exhibit a strongly reduced $Ca_V2.1$ channel activity that is accompanied by an ataxic phenotype. For some of the mutants, it was shown that reduced $Ca_V2.1$ channel activity is accompanied by an altered inhibitory and excitatory synaptic transmission in the cerebellar cortex (*Matsushita et al., 2002; Zhou et al., 2003*), and an increased noise level of Purkinje cell firing (*Hoebeek et al., 2005; Walter et al., 2006*). Total ablation of $Ca_V2.1$ channel activity in conventional *Cacna1a* KO mice, however, resulted in an even more severe phenotype of cerebellar ataxia and early postnatal lethality *(Jun et al., 1999; Fletcher et al., 2001)* and was accompanied by similar abnormalities in cerebellar synaptic transmission (*Miyazaki et al., 2004*).

Because $Ca_V2.1$ channels are expressed in various cerebellar cell types and the abovementioned mutants have abnormal $Ca_V2.1$ channel expression in all synapses, these mutant mice are not helpful in assessing cell type-specific contributions in cerebellar functioning. Here, we applied a genetic approach that specifically removed $Ca_V2.1$-mediated synaptic output from granule cells, which allowed us to investigate the role of these cells in determining the noise level of Purkinje cell firing and downstream motor coordination. To this end, we generated granule cell-specific $Ca_v2.1$ KO mice by crossing recently generated conditional *Cacna1a* mice (*Todorov et al.,* 2006) with transgenic mice expressing Cre recombinase under the granule cell-specific $GABA_A$ receptor α6 subunit promoter (*Aller et al., 2003*). Results from morphological, electrophysiological, and behavioral experiments indicate that $Ca_V2.1$-mediated neurotransmission from cerebellar granule cells is not essential for motor coordination, but is required for regulating the noise level in Purkinje cell firing and consolidation of cerebellar learning.

EXPERIMENTAL PROCEDURES

Animals

Mice with a conditional "floxed" allele of the *Cacna1a* gene (*Todorov et al., 2006*) were bred with $\alpha6^{Cre}$ transgenic mice that express *Cre* recombinase under the cerebellar granule cell-specific $GABA_\alpha$ receptor α6 subunit promoter (*Aller et al., 2003*). In transgenic offspring to which both the floxed allele and the Cre transgene were transmitted, Cre-mediated recombination between loxP sites flanking exon 4 of the *Cacna1a* gene - resulting in deletion of this exon at the genomic level - is expected to occur between postnatal days 7 and 14, when Cre becomes expressed. As a consequence, no functional $Ca_V2.1$ α1 protein will be produced, and therefore no $Ca_V2.1$ channels will be expressed. In homozygous $\alpha6^{Cre}$-*Cacna1a* KO mice, $Ca_V2.1$ channels are not present in cerebellar granule cells, but expression is not affected in other synapses. Genotyping for the presence of the floxed allele was performed by PCR on genomic tail DNA and primers with the following DNA sequence: 5'-acctacagtctgccaggag-3' and 5'-tgaagcccagacatccttgg-3'. For genotyping the *Cre* transgene, primers 5'-acttagcctgggggtaactaaact-3' and 5'-ggtatctctgaccagagtcatcct-3' were used. To

confirm whether Cre-mediated recombination and deletion of exon 4 of *Cacna1a* was successful, primers 5'-agtttctattggacagtgctggt-3' and 5'-ttgcttagcatgcacagg-3' were used. For all experiments, 2- to 8-month-old homozygous $\alpha 6^{Cre}$-*Cacna1a* KO and wild-type littermates were used. All animal experiments were performed in accordance with the guidelines of the respective universities and national legislation.

RT-PCR

Total RNA was isolated from freshly dissected cerebella and frontal cortices from 6-week-old mice according to standard procedures. For RT-PCR, first-strand cDNA was synthesized using random primers, and subsequent PCR was performed using the *Cacna1a*-specific primers 5'-gatgacacggaaccatac-3' and 5'-attgtagaggagatcagtcc-3' that correspond to sequences in exons 3 and 6, respectively.

Immunohistochemistry

Brains from 6-week-old mice were obtained after cardiac perfusion with phosphate-buffered saline and 4% buffered paraformaldehyde, embedded in gelatin, and cut in 40-µm thick sagittal sections. Immunohistochemistry was performed using primary rabbit-anti-calbindin antibody (1:10,000; *CB38*, *SWANT, Bellinzona, Switzerland*) or rabbit-anti-Cre antibody (1:1,000; *AB24608, Abcam, Cambridge, UK*) that were diluted in TBS containing 1% normal horse serum (NHS). Sections were incubated with primary antibody for 2hrs at room temperature and washed in TBS. Subsequently, the sections were incubated with biotinylated goat-anti-rabbit antibody (1:200; *Vector Laboratories, Burlingame, CA, USA)*, diluted in the same buffer, for 1h at room temperature. After washing, the sections were incubated with avidin-biotin-peroxidase complex (*ABC, Vector Laboratories*) and stained with diaminobenzidine (DAB, 0.05%) as a chromogen. Sections were mounted on microscope slides.

Golgi-Cox staining

Brains from-6 week-old mice were isolated after decapitation and processed for Golgi impregnation. Brains were sliced into blocks of approximately 1 cm thickness and rinsed briefly in 0.1 M phosphate buffer (pH 7.4). Tissue was further processed for Golgi-Cox staining using FD Rapid GolgiStain™ Kit (*MTR Scientific, Ijamsville, MD, USA*). Finally, 80 µm-thick sections were cut and mounted on microscope slides. Photographs of the granule cell layer were taken using a microscope with camera of *Leica Microsystems GmbH (Wetzlar, Germany*). The number and length of dendrites were measured using MetaVue software (*Molecular devices, Downingtown, PA, USA*).

Ultrastructural analysis

Brains from 6-week-old mice were obtained after cardiac perfusion with 4% paraformaldehyde and 0.5% glutaraldehyde in cacodylate buffer. After the brains were removed from the skull, they were kept overnight in 4% paraformaldehyde, and cut in

80 µm-thick coronal sections using a vibratome (*Leica Microsystems GmbH*). Sections were then washed and blocked for 1h in 10% NHS and subsequently incubated with rabbit-anti-calbindin antibody (1:7,000; *CB38*, *SWANT*), diluted in TBS containing 2% NHS, for 48 h at 4ºC. Next, sections were incubated overnight at 4ºC in biotinylated goat-anti-rabbit secondary antibody (1:200; *Vector Laboratories*) followed by avidin-biotinylated horseradish peroxidase complex (*Vector Laboratories*). Then the sections were stained with 0.5% DAB and 0.01% H_2O_2 for 15 min at room temperature. Subsequently, the sections were osmicated with 2% osmium in 8% glucose solution, dehydrated in dimethoxypropane, and stained *en block* with 3% uranyl acetate / 70% ethanol for 60 min and embedded in araldite (*Durcupan, Fluka, Deisenhofen, Germany*). Semi-thin 80 µm sections of the cerebellar cortical regions were cut. To analyze granule cell morphology including the synaptic terminals, ultra-thin sections (70-90 nm) were cut using an ultramicrotome (*Leica Microsystems GmbH*), mounted on copper grids, and counterstained with uranyl acetate and lead citrate. The terminals were photographed and analyzed using an electron microscope (*Philips, Eindhoven, The Netherlands*). Electron micrographs were taken at magnifications ranging from 1,500 x to 30,000 x from single-hole EM grids, and analyzed with MetaVue software (*Molecular devices*). The density of the granule cells and their synapses were quantified as the ratio of their number and the total surface analyzed. Surfaces of the granule cell soma, and the postsynaptic densities were measured using the trace region function of the software program. The widths of the synaptic cleft and the parallel fiber terminals were measured by drawing perpendicular lines through the widest part of the object. Finally, the Purkinje cell dendritic spine area was quantified as the product of the height and width of the spine. All data were given as mean values ± SEM.

Intracellular Purkinje cell recordings

In vitro whole-cell patch-clamp recordings of Purkinje cells were performed on adult (3-6 month-old) $\alpha6^{Cre}$-*Cacna1a* KO and wild-type mice, using the method by *Hansel et al.* (2006). In brief, 200 µm-thick sagittal slices from the cerebellar vermis were prepared using a vibratome (*Leica Microsystems GmbH*) while being kept in ice-cold ACSF (containing in mM: 124 NaCl, 5 KCl, 2 $CaCl_2$, 1.25 NaH_2PO_4, 2 $MgSO_4$, 26 $NaHCO_3$ and 15 d-glucose; perfused with 95% O_2 / 5% CO_2). After preparation, the slices were placed at room temperature for > 2hrs before the experiment started. Intracellular patch electrodes (filled with, in mM:, 124 K-gluconate, 9 KCl, 10 KOH, 4 NaCl, 10 HEPES, 28.5 sucrose, 4 Na_2ATP, 0.4 Na_3GTP, pH 7.25-7.35; osmolarity ~290 osm; resistance 2.5 - 3.5 MΩ) and extracellular patch electrodes filled with ACSF were positioned in an experimental bath (*Luigs & Neumann, Ratingen, Germany*) so that the stimulation electrode touched the surface of the slice in the most distal one-third of the molecular layer lateral to the recorded Purkinje cells. Data was amplified, filtered, and stored for off-line analysis using Pulse software *(HEKA, Freiburg, Germany*). Series and input resistances (R_S and R_I, respectively) were monitored by applying a 10-mV hyperpolarizing current step. Recordings were excluded when R_S or R_I varied > 15%

over the course of the experiments, when the holding current > 500 pA, or when the R_I was < 80 MΩ.

Extracellular Purkinje cell recordings

Three 6-month-old mice were prepared for neurophysiological experiments under isoflurane anesthesia using procedures described previously (*Goossens et al., 2001*). In brief, a head-holder was implanted on the skull and a recording chamber was placed over a small hole (< 3 mm) in the occipital bone. During the experiments, the animal was immobilized in a custom-made restrainer by bolting the head-holder to a head-fixation post. Extracellular activity was recorded with glass micropipettes that were advanced into the cerebellar cortex by a hydraulic microdrive equipped with a stepping motor. The raw electrode signal was amplified, filtered, digitized, and stored on disk for off-line analysis. Single-unit Purkinje cell activity was identified by the presence of a brief pause in simple spike (SS) discharge after a complex spike (CS) and was carefully monitored during the course of a recording. Between recording sessions, the brain was covered by ointment and the chamber was sealed using bone wax.

Off-line data analysis was performed in Matlab (*Mathworks Inc., Natick, MA, USA*). The SSs and CSs were detected and discriminated with custom-made software that clustered groups of spikes by means of a linear discriminant analysis on the first four principal components of the spike wave forms (see, e.g., *Eggermont, 1990*). Histograms of SSs triggered upon a CS were made (bin-width was 1 ms) to verify that each isolated Purkinje cell showed a clean climbing fiber pause. Lack of a pause indicated that the cell was not a Purkinje cell or that isolation was imperfect. Spontaneous activity of each Purkinje cell was characterized by: (1) the mean SS and CS firing rate; (2) the SS and CS coefficient of variance (standard deviation of interspike intervals (ISI) / mean of ISI); (3) the climbing fiber pause duration (*Goossens et al., 2001*); and (4) the coefficient of variation of adjacent intervals (CV2; mean value if $(2\times(ISI_{n+1} - ISI_n))/(ISI_{n+1} + ISI_n)$; see also *Holt et al., 1996*).

Rotarod

The accelerating Rotarod (*UGO Basile S.R.L., Commerio VA, Italy*) test was performed on a 4-cm diameter horizontal rotating rod. The test was performed in a semi-dark room with a light source placed at the bottom to discourage the mice from jumping off the rod. Mice (10-22 weeks old) were tested in groups of five. Following a training period (in which the mice were placed on the Rotarod turning at a low constant speed of 5 rpm for 5 min), the mice were subjected to 5 sessions (separated by a 30-min resting period) in a single day. Each trial started with the Rotarod turning at a constant speed of 5 rpm for 10 s, after which the speed was gradually increased to 45 rpm over the following 5 min. The latency to fall (i.e., endurance) was recorded, and the endurance per trial per genotype presented as mean ± SEM.

Erasmus ladder

The Erasmus Ladder is a fully configurable horizontal ladder as previously described (*van der Giessen et al., 2008*). In brief, the horizontal ladder has 37 rungs, covered by a 55 cm × 2.5 cm × 5 cm (l × w × h) tunnel, and has shelters at both ends. Mice (10-22 weeks old) were trained to leave the shelter immediately at the onset of light (i.e., every 10 s) and walk with constant speed to the opposite shelter at 3 pre-training sessions. One pre-training session consisted of 72 trials (i.e., ladder crossings). Mice that did not cross the ladder with a constant speed in these pre-training sessions were excluded from the experiment. Next, for 3 training sessions, a change in walking pattern of the mice was induced as avoidance of an ascending rung either by an unconditioned stimulus (US) or by a conditioned stimulus, i.e. a tone (CS; 15 kHz, 300 ms, 90 dB, smooth onset). Therefore, one of the rungs quickly rose 18 mm, 55 ms after the mouse had touched the preceding rung (randomly chosen rung; mouse walking with constant speed). Each of these three training sessions consisted of 8 blocks of 24 paired trails consisting of 1 US-only trial, 1 CS-only trial, and 1 undisturbed trial (no CS or US present).

Compensatory eye movements

Under general anesthesia (isoflurane ~1.5% and O_2), a pedestal was constructed on the head of the mouse (3-6 months old) parallel to the intracranial midline, using Optibond prime and adhesive (*Kerr, Bioggio, Switzerland*) and Charisma (*Haeraeus Kulzer, Armonk, NY, USA*), modified from *van Alphen & de Zeeuw* (2002). After a recovery period of 2-3 days, the mouse was restrained by means of the two bolts embedded in the pedestal. A cylindrical screen (diam 63 cm) with a random-dotted pattern (each element at 2°) surrounded the turntable (diam 60 cm) on which the mouse was fixed. Two infrared emitters (maximum output 600 mW, dispersion angle 7°, peak wavelength 880 nm) that were fixed on the table, illuminated the eye during the recording, and a third emitter was connected to a camera and aligned horizontally with the camera's optical axis. This third emitter produced the tracked corneal reflection (CR). Eye movements were recorded using the eye-tracking device of *Eye scan systems*.

A calibration of the setup was performed before the recordings started; another was done at the end of each experiment. For this, the camera was rotated several times by ± 10° around the earth-vertical axis passing through the center of the table. The positions of the pupil (P) and corneal reflection (CR) recorded at the extreme positions of the camera rotation were used to calculate Rp, the radius of rotation of the pupil. The gain and phase of the eye movements were calculated using a custom-made Matlab routine (*MathWorks Inc.*). The eye position (E) was calculated using the CR and P positions from the recording, and eye movement computations were performed as described previously (*van Alphen & de Zeeuw, 2002*). For every mouse, we used a 7-day protocol. Day 1 was used for habituation (i.e., half an hour of drum and/or table moving in the dark and in the light). On day 2, baseline recordings were obtained (recordings of OKR

and VVOR followed by the administration of pilocarpine to the eye of the mouse to record also VOR). OKR was recorded over all frequencies (0.1 - 1.6 Hz) with either a fixed amplitude of 5° or a fixed velocity of 8°/s. VOR and VVOR were recorded over the same frequencies with a fixed amplitude of 5°. On day 3, VOR gain-decreas training was provided: VOR was recorded followed by 10 minutes of training in the light during which the drum and the table moved in phase (frequency 0.6 Hz, amplitude drum and table 5°) and another VOR recording at 0.6 Hz only. This sequence was repeated five times. From day 4 to day 7, the VOR phase reversal paradigm was used: VOR recordings were altered with 10 min training blocks during which the table and the drum moved in phase, but the drum amplitude was doubled to 10°. In between sessions, the mice were kept in the dark. At the end of the last session, OKR was recorded to test the effect of the VOR learning paradigm on the visually-driven compensatory eye movements. A frequency of 0.6 Hz was used, so the animal was able to still increase and decrease phase and gain. This protocol was constructed so that three different types of learning could be tested: (1) motor learning during a single, one-hour session; (2) consolidation of this learned motor behaviour; and (3) long-term memory over consecutive days of training.

Data analysis

All values are represented as mean ± standard error of the mean (SEM). p values of < 0.05 were considered significant.

RESULTS

Deletion of exon 4 of *Cacna1a* in cerebellar granule cell neurons

Here, we aimed to ablate $Ca_V2.1$ channels *only* in cerebellar granule cell neurons by crossing mice that were homozygous for a floxed *Cacna1a* allele with homozygous mice expressing Cre recombinase exclusively in cerebellar granule cells. Cre recombinase expression results in recombination of loxP sites flanking exon 4 (*Fig. 1A*), which is expected to lead to no (or abnormal) $Ca_V2.1$ α1 protein and thereby to a lack of $Ca_V2.1$ channels in cerebellar granule cells of homozygous $\alpha6^{Cre}$-*Cacna1a* KO mice. Evidence for Cre-mediated recombination and deletion of *Cacna1a* exon 4 was obtained by RT-PCR, which showed the normal 580 bp PCR product, but also a shorter 490 bp PCR product lacking exon 4 in cerebellar RNA extracts of $\alpha6^{Cre}$-*Cacna1a* KO mice (*Fig. 1B*). Direct sequencing of PCR products verified that exon 4 was deleted (*data not shown*). The absence of a 490 bp product in cerebral tissue indicated that recombination had occurred exclusively in the cerebellum. Further proof of the cell specificity of the recombination was obtained from immunohistochemistry that showed Cre protein expression only in cerebellar granule cells (*Fig. 1C*).

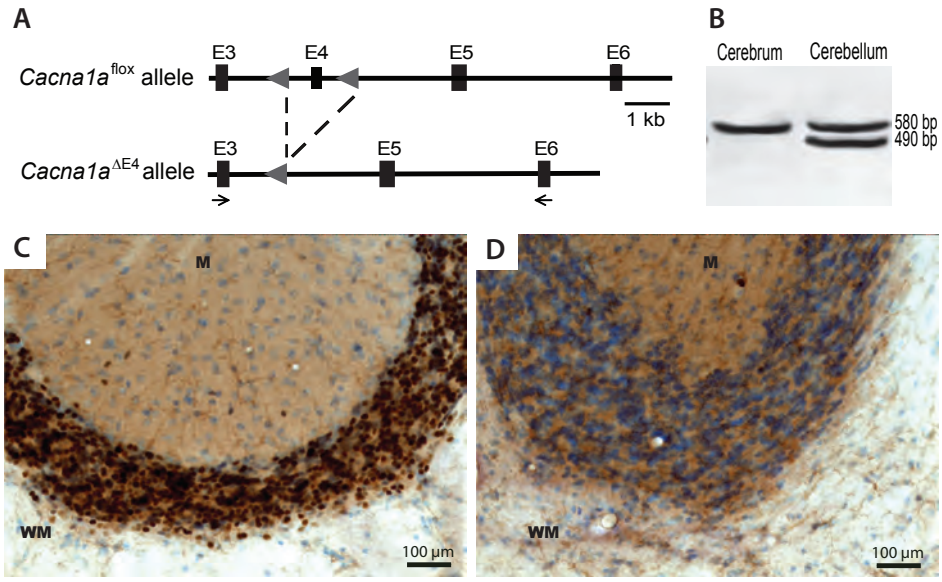

Figure 1. Generation of α6^{Cre}-*Cacna1a* KO mice. (A) Schematic representation of the genomic structure of the relevant part of the *Cacna1a* floxed and deleted alleles showing the location of loxP sites. Black boxes indicate exons (E); triangles indicate the location and direction of the loxP sites; arrows indicate the position of the primers used for RT-PCR in the KO allele. **(B)** RT-PCR of cerebellar and cerebrum total RNA produces a 580-bp product from the floxed *Cacna1a* allele and a 490-bp product from the mutant allele, which lacks exon 4. **(C, D)** Anti-Cre immunostaining of sagittal cerebellar sections reveals relatively high Cre expression (dark color) restricted to granule cells of α6^{Cre}-*Cacna1a* KO mice **(C)**, while no Cre expression is seen in wild type mice **(D)**. Sections are counterstained with methylene blue. WM – white matter; M – molecular layer.

Normal cerebellar and granule cell morphology in α6^{Cre}-*Cacna1a* KO mice

Calbindin staining of cerebellar sections of 6-week-old KO mice did not reveal any overt abnormalities in the cerebellar cytoarchitecture when compared to wild type mice (*Fig. 2A, B*). Moreover, Golgi-Cox-stained cerebellar sections showed that the length and the number of granule cell dendrites did not differ between genotypes (average dendrite length: 14.00 ± 0.67 and. 13.69 ± 0.42 µm, p=0.708 and average number of dendrites: 3.85 ± 0.07 and 3.81 ± 0.07 for wild-type and α6^{Cre}-*Cacna1a* KO mice, respectively; *Fig. 2C, D*). In more detailed structural analyses, no significant difference was observed between wild type and α6^{Cre}-*Cacna1a* KO mice in the average density of granule cells (10.42 ± 028 and 10.16 ± 0.30x10^2 cells/mm^2, p=0.475; *Fig. 3A*), nor in the surface area of granule cell stomata (12.92 ± 0.57 and. 12.73 ± 0.47 mm^2, p=0.805; *Fig. 3B*). The density of parallel fiber synapses (0.54 ± 0.04 and 0.56 ± 0.07 synapses/mm^2 for wild-type and α6^{Cre}-*Cacna1a* KO mice, respectively; p=0.815; *Fig. 3C*) and the surface of the Purkinje cell dendrite spine head (0.13 ± 0.00 and 0.13 ± 0.01 µm^2 for wild-type and α6^{Cre}-*Cacna1a* KO, respectively; p=0.964; *Fig. 3F*) were similar between the genotypes. In contrast, an almost significant increase was

observed in the width of the granule cell axonal terminals in KO mice (0.75 ± 0.03 and 0.91 ± 0.06 µm for wild-type and α6^{Cre}-*Cacna1a* KO, respectively; p=0.057; *Fig. 3D*). The surface of the postsynaptic density was also slightly smaller in α6^{Cre}-*Cacna1a* KO mice (8.07 ± 0.28 ×10^{-3} nm^2) than in wild-type mice (7.38 ± 0.09 × 10^{-3} nm^2; p=0.059; *Fig. 3E*). These findings indicate that although the lack of $Ca_v2.1$ channels from the granule cells may alter, to some extent, their axonal terminals, it does not result in changes in granule cell or overall cerebellar morphology.

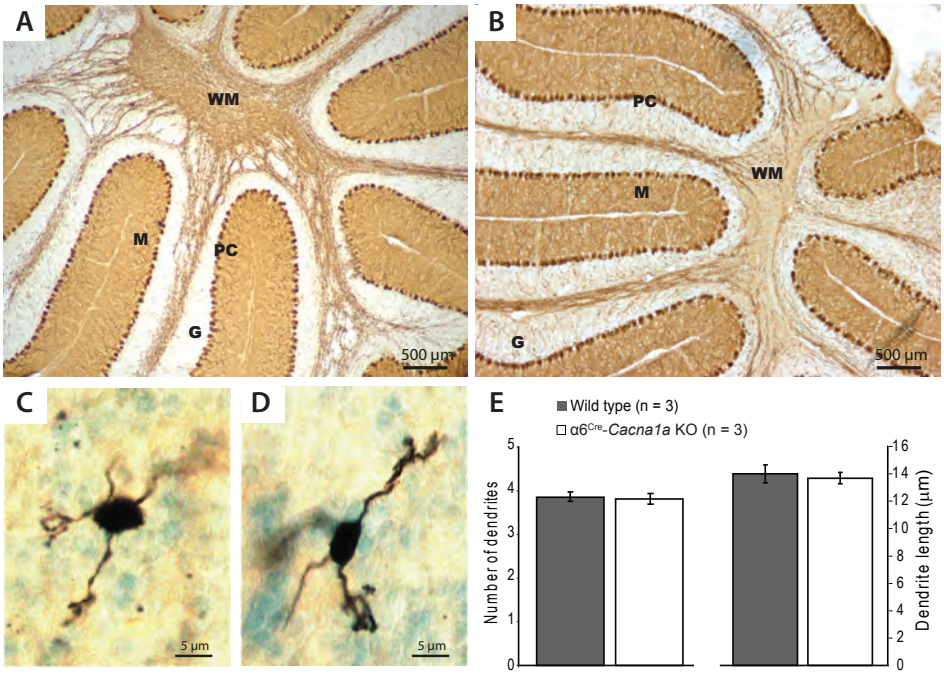

Figure 2. Normal overall cytoarchitecture of the cerebellum and basic morphology of cerebellar granule cells α6^{Cre}-*Cacna1a* KO mice. (A, B) Anti-calbindin stained sagittal sections from the cerebellum of α6^{Cre}-*Cacna1a* KO (**A**) and wild-type (**B**) mice reveal normal foliation and cytoarchitecture. PC – Purkinje cell layer; WM – white matter; G – granule cell layer; M – molecular layer. **(C, D)** Golgi-Cox stained granule cell of α6^{Cre}-*Cacna1a* KO (**C**) and wild type (D) mouse presenting with normal structure and arborization. **(E)** Light microscopy quantification of the number and length of granule cell dendrites in α6^{Cre}-*Cacna1a* KO and wild-type mice.

In vitro electrophysiology shows that synaptic transmission at PF-PC synapses is reduced in α6^{Cre}-*Cacna1a* KO mice

To study the effects of granule cell-specific ablation of $Ca_v2.1$ channels on the efficacy of granule cell output, whole-cell patch-clamp recordings of Purkinje cells were performed in vermal slices of adult mice (3-6 months old). These recordings showed that when parallel fibers were activated, the excitatory postsynaptic currents (EPSCs) in Purkinje

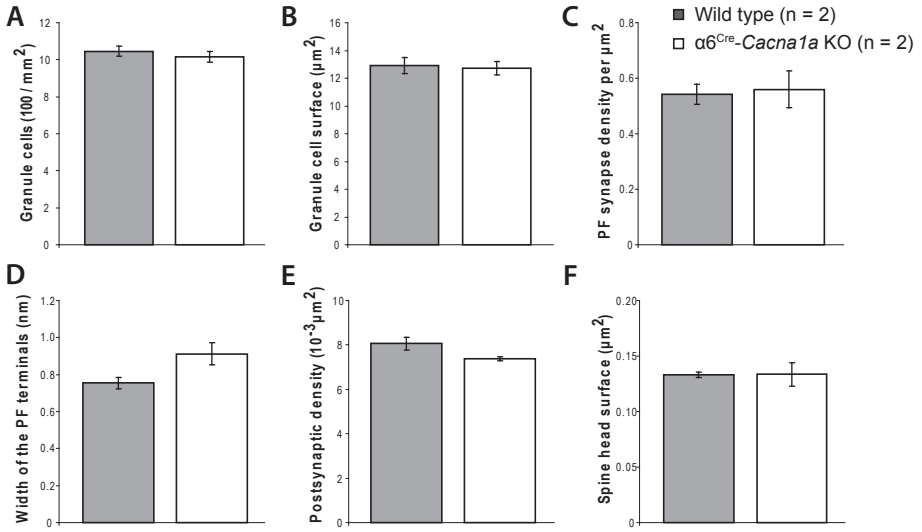

Figure 3. Electron microscopical quantification reveals no changes in morphology of parallel fiber-Purkinje cell synapses of α6^{Cre}-*Cacna1a* KO mice. No significant difference was observed in α6^{Cre}-*Cacna1a* KO and wild-type mice with respect to **(A)** the density of the granule cells (p=0.475), **(B)** the surface area of granule cells (p = 0.805), **(C)** the density of the parallel fiber synapses (p=0.815), **(D)** the width of the parallel fiber synaptic terminals (p = 0.057), **(E)** the surface area of the postsynaptic density (p=0.059), and **(F)** the surface area of Purkinje cell dendrite spine heads (p=0.964).

cells were dramatically reduced (up to 65%, depending on the stimulus intensity) in α6^{Cre}-*Cacna1a* KO compared to wild-type mice (repeated measures ANOVA p<0.001; *Fig. 4A*), which is in line with the expected decreased $Ca_V2.1$-mediated Ca^{2+} influx in parallel fiber synapses (*Mintz et al., 1995*). A decrease in presynaptic Ca^{2+} influx is also likely to affect synaptic plasticity. To investigate presynaptic short-term plasticity at the PF-PC synapse, we recorded paired-pulse facilitation of the EPSCs in Purkinje cells. Much to our surprise, no significant difference (p=0.3) was observed between genotypes *(Fig. 4B)*, which indicates that there is no dramatic change in presynaptic handling of residual Ca^{2+}-ions between two stimuli. Thus, despite decreased synaptic efficacy at PF-PC synapses, presynaptic short-term plasticity is preserved in α6^{Cre}-*Cacna1a* KO mice. The morphological and electrophysiological data together indicate that in α6^{Cre}-*Cacna1a* KO mice, synaptic transmission at the PF-PC synapse is disturbed due to a decrease in neurotransmitter release.

In vivo electrophysiology reveals lower noise level in Purkinje cell simple spike firing in α6^{Cre}-*Cacna1a* KO mice

To further investigate the effects of decreased neurotransmitter release at PF-PC synapses, Purkinje cell activity was measured *in vivo* in awake mice (see *Hoebeek et al., 2005*). In both wild-type and α6^{Cre}-*Cacna1a* KO mice, Purkinje cell firing patterns were characterized by simple spike (i.e., indicative of intrinsic excitability as well as

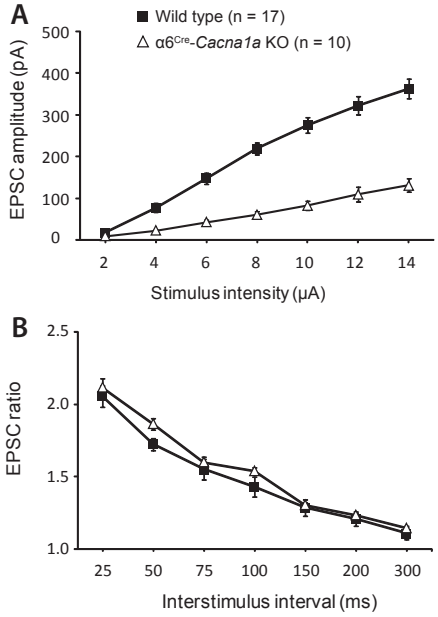

Figure 4. Neurotransmission is decreased at parallel fiber-Purkinje cell synapses of α6^{Cre}-*Cacna1a* KO mice. (A) Excitatory postsynaptic currents (EPSCs) in Purkinje cells are dramatically smaller in α6^{Cre}-*Cacna1a* KO than in wild-type mice (p<0.001). **(B)** Paired-pulse facilitation of the EPSCs in Purkinje cells revealed no significant differences between α6^{Cre}-*Cacna1a* KO and wild-type mice (p=0.3).

excitatory and inhibitory input) and complex spike activity (indicative of activity in the inferior olivary nucleus) (*Fig. 5A, B*). Quantification of these firing patterns showed that reduced synaptic transmission of granule cells upon Purkinje cell did not result in a decreased simple spike firing frequency in KO mice (56.4 ± 2.3 and 59.2 ± 4.4 Hz in KO and wild type mice, respectively; p=0.2; *Fig. 5C*). Moreover, also the overall regularity of firing, as assessed by calculating the coefficient of variance (CV) for all inter-spike intervals ([standard deviation of all inter-spike intervals] / [mean of all inter-spike intervals]), showed no significant difference between genotypes (0.5 ± 0.1 and 0.6 ± 0.1 for α6^{Cre}-*Cacna1a* KO and wild-type mice, respectively; p=0.3).

However, when the simple spike temporal patterning was investigated by calculating the CV for adjacent inter-spike intervals (CV_2; mean value of $(2*|ISI_{n+1} - ISI_n|) / (ISI_{n+1} + ISI_n)$; see *Holt et al., 1996*), the simple spike firing pattern of α6^{Cre}-*Cacna1a* KO mice appeared to be significantly *more regular* than that of wild-type mice (median CV_2: 0.25 ± 0.01 and 0.31 ± 0.03; p=0.03; mean CV_2: 0.32 ± 0.01 and 0.37 ± 0.03; p=0.08; *Fig. 5D*). These results show that the noise levels in simple spike firing are lower in the Purkinje cells of α6^{Cre}-*Cacna1a* KO than that of wild-type mice. To further study the properties of Purkinje cells, the firing pattern of the complex spikes was analyzed and revealed a normal firing frequency (0.97 ± 0.05 and 1.01 ± 0.08 Hz for α6^{Cre}-*Cacna1a* KO and wild-type, respectively; p=0.4; *Fig. 5E*) and regularity (0.84 ± 0.04 and 0.84 ± 0.06 for α6^{Cre}-*Cacna1a* KO and wild-type, respectively; p=0.9) in KO mice. In conclusion, besides a decrease in simple spike noise levels, no other alterations were observed in Purkinje cell firing patterns in α6^{Cre}-*Cacna1a* KO mice.

Motor performance is not affected in α6^{Cre}-*Cacna1a* KO mice

Theoretically, the decreased synaptic transmission at the PF-PC synapse and the abnormal Purkinje cell firing patterns could have resulted in motor discoordination. However, no overt signs of ataxia were observed in homozygous α6^{Cre}-*Cacna1a* KO

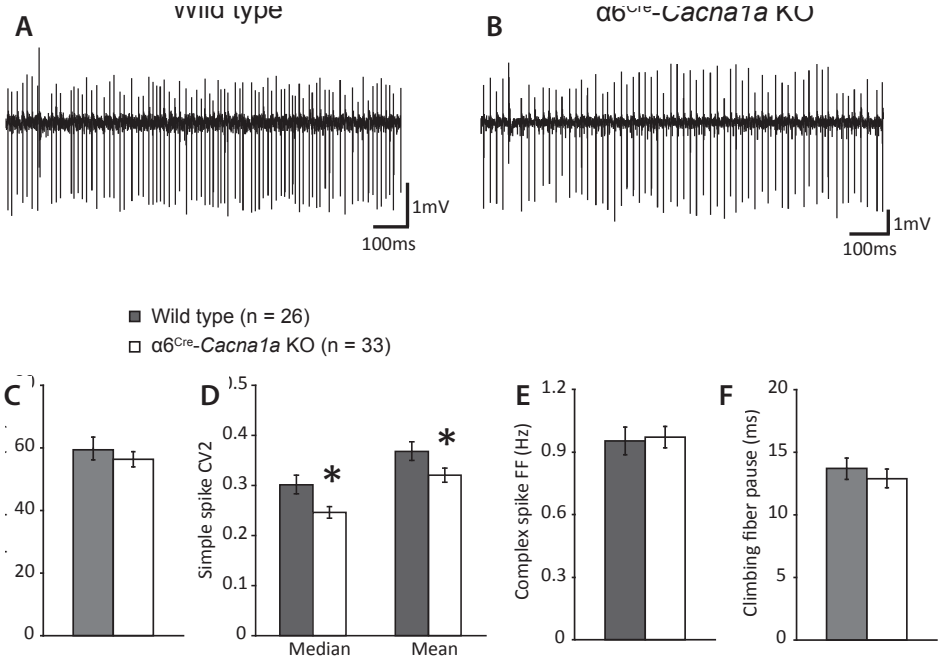

Figure 5. Decreased irregularity of Purkinje cells *in vivo* simple spike firing in α6^{Cre}-*Cacna1a* mice. Extracellular recordings of spontaneous Purkinje cell activities of a wild-type **(A)** and a α6^{Cre}-*Cacna1a* KO mouse **(B)**. Note the increased irregularity of the simple spikes in α6^{Cre}-*Cacna1a* KO mice. Complex spikes are positive and simple spikes are negative. **(C)** The mean simple spike firing rates were not significantly different between the two genotypes (p=0.2). **(D)** Both the mean and the median coefficients of variation of adjacent intervals (CV2) of ISIs were significantly lower in α6^{Cre}-*Cacna1a* KO than in wild-type Purkinje cells. **(E)** The Purkinje cell complex spike firing frequency was normal and did not differ betweent he two groups (p=0.4). **(F)** No differences were noted in the climbing fiber pause in Purkinje cell firing pattern between the two genotypes (p>0.05). Asterisks indicate significance between genotypes.

mice when housed in their home cage. This was confirmed by more general motor performance tests, i.e., accelerating rotarod and Erasmus ladder (*Fig. 6A, B*) that did not reveal significant differences between genotypes (all p values > 0.2). Next, we tested the compensatory eye movements according to standard procedures (see *Wulff et al., 2009*). Both the amplitude (gain) and timing (phase) of the optokinetic reflex (OKR) and vestibulo-ocular reflex in the dark (VOR) and light (visually-enhanced VOR; VVOR) were recorded, but revealed no significant differences between genotypes (*Fig 6C-H*). Apparently, severe disturbance of the synaptic transmission at the PF-PC synapse does not alter motor performance.

Consolidation of motor learning is affected in α6^{Cre}-*Cacna1a* KO mice

The PF-PC synapse has been ascribed a central role in regulating many forms of motor learning, such as VOR adaptation (*Ito, 2001*), which may be affected in α6^{Cre}-*Cacna1a*

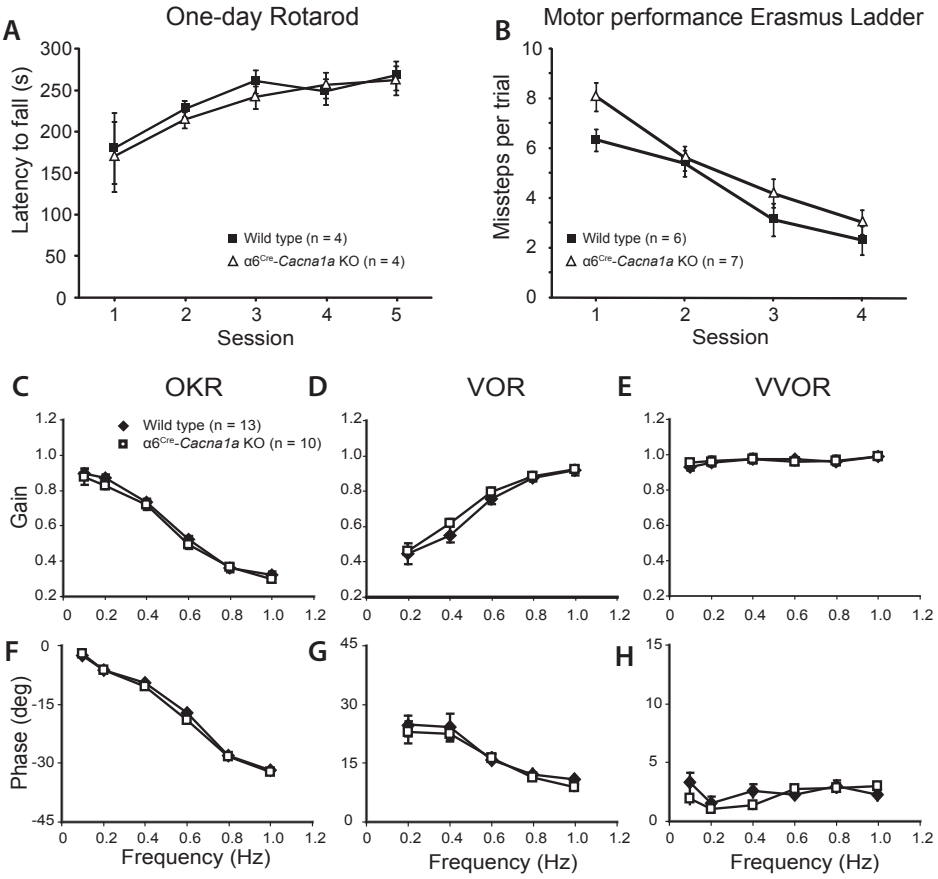

Figure 6. General motor coordination is not affected in α6^{Cre}-*Cacna1a* KO mice. Accelerating rotarod **(A)** and Erasmus ladder **(B)** result showed normal motor coordination of α6^{Cre}-*Cacna1a* KO mice. **(C-H)** Baseline values for optokinetic reflex (OKR), vestibulo-ocular reflex in dark (VOR), and and in light (VVOR) are provided for α6^{Cre}-*Cacna1a* KO and wild-type mice. Motor coordination during the OKR (**C, F**) and during the VOR(**D, G**) and the VVOR (**E, H**). Stimulus frequencies of the optokinetic drum and turntable were varied from 0.1 Hz to 1.0 Hz. Stimulus amplitude was fixed at 5° for both the drum and the table. No significant differences were observed between α6^{Cre}-*Cacna1a* KO and wild-type mice (p>0.05).

mice given the decreased synaptic transmission at this synapse. To test this, we used a VOR training paradigm aimed at reducing the gain of the VOR (on day 1) and subsequently reversing its phase (on the following days; days 2-5) (modified from *van Alphen & de Zeeuw, 2002*). Short-term adaptation was tested each day by recording the response to an in-phase rotation of both the visual field and the mouse every 10 minutes, whereas long-term adaptations were studied comparing the results at the end of the sessions at day 5 with the values at the beginning of day 2. The paradigm at day 1 included in-phase rotation of 5° at 0.6 Hz and did not result in a significant difference in gain reduction between α6^{Cre}-*Cacna1a* KO and wild-type mice (p=0.91 by repeated-measures ANOVA; *Fig. 7A, B*). However, when the measurements were resumed the

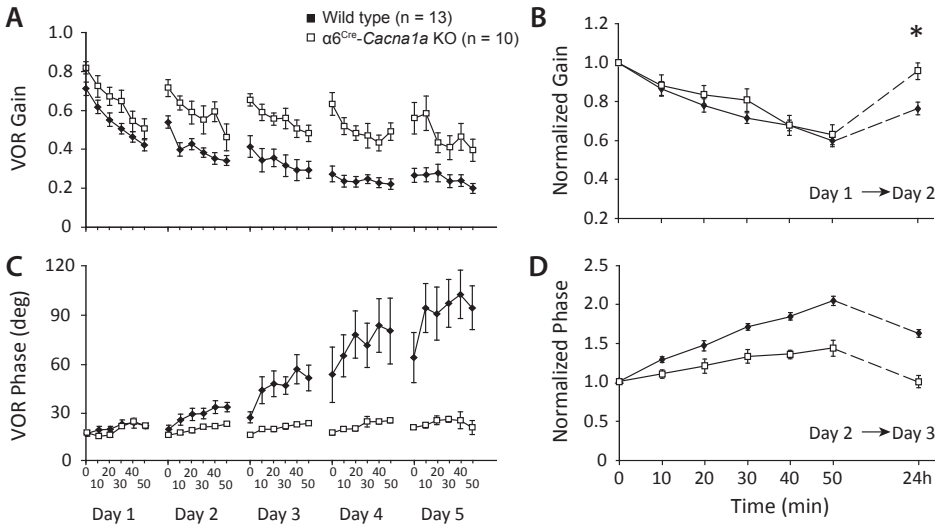

Figure 7. α6^{Cre}-*Cacna1a* mice were fully capable of learning motor tasks, but fail to consolidate learning over time. (A, B) VOR gain values at 0.6 Hz, which were recorded every 10 minutes during training are given. (**C, D**) VOR phase values recorded at 0.6 Hz every 10 minutes during each training session are given. Note that the separate training days were consecutive and that the mice were kept for 24 hours in the dark in between training sessions. Asterisk indicates significance between genotypes.

next day, the degree of gain reduction carried forward from the previous day's learning was significantly *smaller* in α6^{Cre}-*Cacna1a* KO mice (p=0.023 by t-test; *Fig. 7B*).

Thus, whereas α6^{Cre}-*Cacna1a* KO mice showed a relatively normal capacity for gain decrease, they lacked the ability to consolidate this newly learned motor behavior. Between the second and third day of recordings, the same effect on the consolidation of phase changes was observed (p<0.01 by t-test). The inability to remember the training paradigm of the previous day became particularly evident as KO mice were unable to reverse the phase of their VOR during training days 2-5 (*Fig. 7C, D*). These data indicate that normal synaptic transmission at cerebellar granule cell synapses is essential for the consolidation of VOR learning paradigms that decrease the gain and/or reverse the phase. In other words, modulating the noise levels in Purkinje cell simple spike firing by granule cell activity is necessary for the consolidation of motor learning.

DISCUSSION

During this study we made use of the possibilities of conditional gene targeting to generate α6^{Cre}-*Cacna1a* KO mice in which $Ca_V2.1$ channels were selectively ablated in cerebellar granule cell neurons. This approach allowed us to study, for the first time, the specific contribution of these neurons to motor behavior. Cerebellar granule

cells have been thought to convey mossy fiber input to the cerebellum by providing excitatory input to their target neurons (i.e., Purkinje cells) and thereby regulate their firing frequency. Here, we could show that when granule cell output is reduced, the output of the cerebellar cortex is still functionally intact in the sense that the firing frequency of Purkinje cells remained unchanged and that motor coordination was not affected. A detailed study of Purkinje cell firing patterns, however, revealed that, at the millisecond timescale, the interspike intervals are more regular in the $\alpha6^{Cre}$-*Cacna1a* KO, which was the only relevant change, and therefore must be related to the decrease in consolidation of motor learning in these mice.

Specificity of the cell-specific $Ca_V2.1$ channel ablation

Ablation of $Ca_v2.1$ channels *specifically* in granule cells was achieved through *in vivo* genetic recombination by crossing conditional *Cacna1a* mice (*Todorov et al., 2006*) with transgenic mice expressing Cre recombinase, driven by the granule cell-specific $GABA_A$ receptor α6 subunit promoter (*Aller et al., 2003*). This strategy circumvented several limitations that the use of conventional $Ca_V2.1$ KO mice have, i.e. the widespread effects resulting from the lack of functional $Ca_V2.1$ channels throughout the peripheral and central nervous systems of these mice, often compensated for by an upregulation of other Ca_V channels. In addition, the homozygous $Ca_V2.1$ KO exhibit early postnatal lethality around postnatal day 20, making investigations in adult mice impossible (*Jun et al., 1999; Fletcher et al., 2001; Kaja et al., 2007*).

Granule cell specificity was already shown by *Aller et al.* (*2003*) and confirmed in this study by molecular analyses in $\alpha6^{Cre}$-*Cacna1a* KO mice. Functional evidence for the lack of $Ca_V2.1$ channels in granule cells came from the dramatically reduced neurotransmitter release at PF-PC synapses that to a large extent is dependent on $Ca_V2.1$-mediated neuronal Ca^{2+} influx. Together, these data provide evidence that $Ca_V2.1$ channel ablation in $\alpha6^{Cre}$-*Cacna1a* KO mice is indeed granule cell-specific.

Possible effect of granule cell-specific *Cacna1a* deletion on interneuron activity

Granule cells not only provide direct input on Purkinje cells through parallel fiber synapses, but also indirectly contact Purkinje cells via inhibitory interneurons (i.e., the stellate and basket cells) of the molecular layer. Ablation of $Ca_V2.1$ in granule cells may therefore also affect the input on and modulation of Purkinje cell firing via the indirect route. Possible consequences for the findings in this study cannot be ignored.

Given the reduced neurotransmission in PF-PC synapses in $\alpha6^{Cre}$-*Cacna1a* KO mice, it is not unlikely that the granule cell input to interneurons is also decreased. Granule cell input on Purkinje cells is a balance between excitatory input from parallel fibers and inhibitory input from the interneurons. So, if both synapse types are equally affected, a decrease in excitatory neurotransmission through parallel fibers can be compensated for by the reduced firing frequency of stellate and basket cells. This would theoretically result in a net unchanged synaptic input on the Purkinje cells in $\alpha6^{Cre}$-*Cacna1a* KO

mice. However, there is circumstantial evidence that the inhibitory input to Purkinje cells is not compromised. The main reason for this is that our current data show that Purkinje cells, which - like stellate and basket cells (*Midtgaard, 1992*) - are intrinsically active (*Llinas and Sugimori, 1980*), do not show a decrease in their average firing frequency, regardless of the decrease in their excitatory synaptic input. This argues against a concomitant decrease in the firing frequency of inhibitory interneurons in $\alpha6^{Cre}$-*Cacna1a* KO mice. However, experiments investigating granule cell synaptic transmission to stellate and basket cells (as well as their firing patterns) are needed to assess whether inhibitory interneurons may play a role in determining Purkinje cell firing patterns in the $\alpha6^{Cre}$-*Cacna1a* KO mice.

Motor coordination in $\alpha6^{Cre}$-*Cacna1a* KO mice is unaffected despite strongly reduced PF-PC synaptic transmission

Rather unexpected, $\alpha6^{Cre}$-*Cacna1a* KO mice do not show motor performance abnormalities on the accelerating rotarod or the Erasmus ladder, despite an up-to-65% decrease in synaptic transmission at the PF-PC synapse, which is the most prevalent cerebellar synapse. Compensatory mechanisms, such as increasing the density of PF-PC synapses or other alterations in the morphological and/or electrophysiological properties as seen in *tottering* mice that have a strongly reduced $Ca_V2.1$ channel current density (*Zhou et al., 2003*), could have occurred, leading to a "novel balance" between excitatory and inhibitory input onto Purkinje cells. Remarkable, no changes in either the density of parallel fiber synapses or the number of Purkinje cell dendrite spines contacting a single varicosity were observed in $\alpha6^{Cre}$-*Cacna1a* KO mice. Also, these mice did not reveal gross abnormalities in the morphology of the cerebellum or granule neurons, except for a slight, but not significant, increase in the width of the PF-PC synaptic terminals.

Previously, it was shown that an increase in the Purkinje cell noise levels in *tottering* mice, which have a decreased $Ca_V2.1$ channel function throughout the cerebellar cortex, results in ataxia, probably because of the reduction in information content in the cerebellar output (*Hoebeek et al., 2005*). Here, we demonstrated that a decrease in simple spike noise levels can occur without causing ataxia. It suggests that motor coordination is unaffected when Purkinje cell noise levels are decreased, whereas an increase in these levels results in severe motor coordination problems. Furthermore, we could demonstrate that decreased Purkinje cell noise levels did not affect motor learning itself, but rather compromised the consolidation of motor learning. This implies that consolidation of motor learning itself must happen downstream of the cerebellar cortex and is therefore dependent on the output of the cerebellar cortex.

REFERENCES

1. Aller MI, Jones A, Merlo D, Paterlini M, Meyer AH, Amtmann U, Brickley S, Jolin HE, McKenzie AN, Monyer H, Farrant M, Wisden W. Cerebellar granule cell Cre recombinase expression. Genesis. 2003;36:97-103.
2. Barclay J, Balaguero N, Mione M, Ackerman SL, Letts VA, Brodbeck J, Canti C, Meir A, Page KM, Kusumi K, Perez-Reyes E, Lander ES, Frankel WN, Gardiner RM, Dolphin AC, Rees M. Ducky mouse phenotype of epilepsy and ataxia is associated with mutations in the Cacna2d2 gene and decreased calcium channel current in cerebellar Purkinje cells. J Neurosci. 2001;21:6095-104.
3. Fletcher CF, Lutz CM, O'Sullivan TN, Shaughnessy JD Jr, Hawkes R, Frankel WN, Copeland NG, Jenkins NA. Absence epilepsy in tottering mutant mice is associated with calcium channel defects. Cell.1996;87:607-17.
4. Fletcher CF, Tottene A, Lennon VA, Wilson SM, Dubel SJ, Paylor R, Hosford DA, Tessarollo L, McEnery MW, Pietrobon D, Copeland NG, Jenkins NA. Dystonia and cerebellar atrophy in Cacna1a null mice lacking P/Q calcium channel activity. FASEB J. 2001;15:1288-90.
5. Glickstein M. Mossy-fibre sensory input to the cerebellum. Prog Brain Res. 1997; 114:251-9.
6. Goossens J, Daniel H, Rancillac A, van der Steen J, Oberdick J, Crépel F, De Zeeuw CI, Frens MA. Expression of protein kinase C inhibitor blocks cerebellar long-term depression without affecting Purkinje cell excitability in alert mice. J Neurosci. 2001;21:5813-23.
7. Goossens HH, Hoebeek FE, Van Alphen AM, Van Der Steen J, Stahl JS, De Zeeuw CI, Frens MA. Simple spike and complex spike activity of floccular Purkinje cells during the optokinetic reflex in mice lacking cerebellar long-term depression. Eur J Neurosci. 2004;19:687-97.
8. Hansel C, de Jeu M, Belmeguenai A, Houtman SH, Buitendijk GH, Andreev D, De Zeeuw CI, Elgersma Y. AlphaCaMKII Is essential for cerebellar LTD and motor learning. Neuron. 2006;51:835-43.
9. Häusser M, Clark BA. Tonic synaptic inhibition modulates neuronal output pattern and spatiotemporal synaptic integration. Neuron. 1997;19:665-78.
10. Hoebeek FE, Stahl JS, van Alphen AM, Schonewille M, Luo C, Rutteman M, van den Maagdenberg AM, Molenaar PC, Goossens HH, Frens MA, De Zeeuw CI. Increased noise level of Purkinje cell activities minimizes impact of their modulation during sensorimotor control. Neuron. 2005;45:953-65.
11. Hoebeek FE, Khosrovani S, Witter L, De Zeeuw CI. Purkinje cell input to cerebellar nuclei in tottering: ultrastructure and physiology. Cerebellum. 2008;7:547-58.
12. Holt GR, Softky WR, Koch C, Douglas RJ. Comparison of discharge variability in vitro and in vivo in cat visual cortex neurons. J Neurophysiol. 1996;75:1806-14.
13. Ito M. Cerebellar long-term depression: characterization, signal transduction, and functional roles. Physiol Rev. 2001;81:1143-95.
14. Jun K, Piedras-Rentería ES, Smith SM, Wheeler DB, Lee SB, Lee TG, Chin H, Adams ME, Scheller RH, Tsien RW, Shin HS. Ablation of P/Q-type Ca(2+) channel currents, altered synaptic transmission, and progressive ataxia in mice lacking the alpha(1A)-subunit. Proc Natl Acad Sci U S A. 1999;96:15245-50.
15. Kaja S, van de Ven RC, Broos LA, Frants RR, Ferrari MD, van den Maagdenberg AM, Plomp JJ. Characterization of acetylcholine release and the compensatory contribution of non-Ca(v)2.1 channels at motor nerve terminals of leaner Ca(v)2.1-mutant mice. Neuroscience. 2007;144:1278-87.
16. Llinás R, Sugimori M. Electrophysiological properties of in vitro Purkinje cell dendrites in mammalian cerebellar slices. J Physiol. 1980;305:197-213.
17. Llinás RR, Sugimori M, Cherksey B. Voltage-dependent calcium conductances in mammalian neurons. The P channel. Ann N Y Acad Sci. 1989;560:103-11.
18. Liu S, Friel DD. Impact of the leaner P/Q-type Ca2+ channel mutation on excitatory synaptic transmission in cerebellar Purkinje cells. J Physiol. 2008;586:4501-15
19. Matsushita K, Wakamori M, Rhyu IJ, Arii T, Oda S, Mori Y, Imoto K. Bidirectional alterations in cerebellar synaptic transmission of tottering and rolling Ca2+ channel mutant mice. J Neurosci. 2002;22:4388-98.
20. Midtgaard J. Stellate cell inhibition of Purkinje cells in the turtle cerebellum in vitro. J Physiol. 1992;457:355-67.
21. Mintz IM, Sabatini BL, Regehr WG. Calcium control of transmitter release at a cerebellar synapse. Neuron. 1995;15:675-88.
22. Mittmann W, Koch U, Häusser M. Feed-forward inhibition shapes the spike output of cer-

ebellar Purkinje cells. J Physiol. 2005;563:369-78.

23. Miyazaki T, Hashimoto K, Shin HS, Kano M, Watanabe M. P/Q-type Ca2+ channel alpha1A regulates synaptic competition on developing cerebellar Purkinje cells. J Neurosci. 2004;24:1734-43.
24. Mori Y, Wakamori M, Oda S, Fletcher CF, Sekiguchi N, Mori E, Copeland NG, Jenkins NA, Matsushita K, Matsuyama Z, Imoto K. Reduced voltage sensitivity of activation of P/Q-type Ca2+ channels is associated with the ataxic mouse mutation rolling Nagoya (tg(rol)). J Neurosci. 2000;20:5654-62.
25. Schonewille M, Luo C, Ruigrok TJ, Voogd J, Schmolesky MT, Rutteman M, Hoebeek FE, De Jeu MT, De Zeeuw CI. Zonal organization of the mouse flocculus: physiology, input, and output. J Comp Neurol. 2006;497:670-82.
26. Steuber V, Mittmann W, Hoebeek FE, Silver RA, De Zeeuw CI, Häusser M, De Schutter E. Cerebellar LTD and pattern recognition by Purkinje cells. Neuron. 2007;54:121-36.
27. Todorov B, van de Ven RC, Kaja S, Broos LA, Verbeek SJ, Plomp JJ, Ferrari MD, Frants RR, van den Maagdenberg AM. Conditional inactivation of the Cacna1a gene in transgenic mice. Genesis. 2006;44:589-94.
28. Van Alphen AM, De Zeeuw CI. Cerebellar LTD facilitates but is not essential for long-term adaptation of the vestibulo-ocular reflex. Eur J Neurosci. 2002;16:486-90.
29. Van Der Giessen RS, Koekkoek SK, van Dorp S, De Gruijl JR, Cupido A, Khosrovani S, Dortland B, Wellershaus K, Degen J, Deuchars J, Fuchs EC, Monyer H, Willecke K, De Jeu MT, De Zeeuw CI. Role of olivary electrical coupling in cerebellar motor learning. Neuron. 2008;58:599-612.
30. Voogd J, Glickstein M. The anatomy of the cerebellum. Trends Neurosci. 1998;21:370-5.
31. Wada N, Kishimoto Y, Watanabe D, Kano M, Hirano T, Funabiki K, Nakanishi S. Conditioned eyeblink learning is formed and stored without cerebellar granule cell transmission. Proc Natl Acad Sci U S A. 2007;104:16690-5.
32. Wakamori M, Yamazaki K, Matsunodaira H, Teramoto T, Tanaka I, Niidome T, Sawada K, Nishizawa Y, Sekiguchi N, Mori E, Mori Y, Imoto K. Single tottering mutations responsible for the neuropathic phenotype of the P-type calcium channel. J Biol Chem. 1998;273:34857-67.
33. Walter JT, Alviña K, Womack MD, Chevez C, Khodakhah K. Decreases in the precision of Purkinje cell pacemaking cause cerebellar dysfunction and ataxia. Nat Neurosci. 2006; 9:389-97.
34. Wulff P, Schonewille M, Renzi M, Viltono L, Sassoè-Pognetto M, Badura A, Gao Z, Hoebeek FE, van Dorp S, Wisden W, Farrant M, De Zeeuw CI. Synaptic inhibition of Purkinje cells mediates consolidation of vestibulo-cerebellar motor learning. Nat Neurosci. 2009;12:1042-9.
35. Zhang JF, Randall AD, Ellinor PT, Horne WA, Sather WA, Tanabe T, Schwarz TL, Tsien RW. Distinctive pharmacology and kinetics of cloned neuronal Ca2+ channels and their possible counterparts in mammalian CNS neurons. Neuropharmacology. 1993;32:1075-88.
36. Zhou YD, Turner TJ, Dunlap K. Enhanced G protein-dependent modulation of excitatory synaptic transmission in the cerebellum of the Ca2+ channel-mutant mouse, tottering. J Physiol. 2003; 547:497-507.